JOURNAL OF PROPULSION AND POWER
Vol. 14, No. 6, November–December 1998

Automated Optimal Design of Two-Dimensional Supersonic Missile Inlets

Michael Blaize,* Doyle Knight,† and Khaled Rasheed‡
Rutgers University, New Brunswick, New Jersey 08903

A new methodology has been developed for the automated optimal design of two-dimensional high-speed inlets. A semiempirical flow solver and an improved genetic algorithm are linked within an automated loop. The purpose of this process is to maximize the total pressure recovery of the missile inlet: first of all, for one upstream flow condition, and secondly, for an entire mission. This innovative design strategy allows great improvement of the original inlet design in a very short period of time. Successful results are presented for optimizations of inlets originally designed and tested at the Institute of Theoretical and Applied Mechanics in Novosibirsk, Russia. The significant improvements of the total pressure recovery, achieved by the automated optimization loop, are verified using a full Navier–Stokes solver.

I. Introduction

DESIGN optimization in aerodynamics and propulsion has always been of great interest and has, therefore, received much attention.[1] The direct result of improvement in computer technology is the growing interest in automated design techniques aimed at achieving better designs in a shorter period of time than classical methods, i.e., by hand or extensive analysis.

Optimization techniques can be classified into three different categories: local, global, and other methods. The first category is gradient-based algorithms that use local information to search part of the design space and find the local minimum. (An optimization problem can be recast as a minimization problem with no loss of generality. For example, maximizing a function f is equivalent to minimizing $-f$.) These methods are able to solve nonlinear problems together with inequality and equality constraints. Many local methods are available,[2,3] e.g., adjoint, single, or multigrid preconditioners, alternating direction implicit methods, control theory,[4] etc. These methods are fast and accurate; however, they are typically unable to find the global optimum of the entire design space and are inefficient in discrete design spaces.

The second category is stochastic algorithms that attempt to take into consideration the whole search space. There are many different schemes; however, they all incorporate some amount of randomness. This category includes the genetic algorithms (GAs), simulated annealing, pseudotime methods, random search, etc. These global methods are more likely to converge toward a global optimum rather than a local one. Furthermore, they are able to deal with discontinuous design spaces.[5] However, these kinds of optimization techniques are more expensive in computational time than the first category because they typically require substantially more design evaluations. Among the global methods, the most successful and popular to date are GA.[6,7] They are based upon evolutionary principles and will be described in further detail in Sec. II. Other optimization techniques are available and do not enter into the previously defined categories. Examples are one-shot methods[8] or inverse methods.[9,10]

Optimization techniques have been applied to a wide range of design problems, from conceptual design to multidisciplinary design optimization (MDO). Within the aerospace industry, optimization techniques have made a significant contribution to the design of highly complicated systems involving many design parameters and constraints. Both local and global methods have been used, depending on the design space and the aim of the user. Wing design was one of the first areas of application of optimization procedures. Typically, the objective is to achieve a low-drag and high-lift wing, together with structural or geometric constraints. References 11–22 relate some of the previous works in this field. In the propulsion domain some previous works have been carried out with gradient-based optimizers that were successfully used for designing or redesigning of hypersonic and supersonic intakes and nozzles.[23–29] Missile shapes have also been considered through optimization.[30]

The actual trend is to use several analysis tools and broaden the design optimization so that the optimization becomes multidisciplinary.[31,32] Furthermore, engineers are looking forward to including more artificial intelligence into the optimization methods with a view to achieving faster convergence toward the global optimum.[33] In addition to the automated optimization of numerical simulators, some works have been performed in the field of automated optimization of experimental tests.[34,35]

Considering previous works that were carried out on inlet optimization and the characteristic of the analysis tool used in this study, GA was chosen to perform the optimization of a two-dimensional inlet using a semiempirical flow solver as the simulation tool. The objective of this paper is to demonstrate a strategy for the automated optimal design of inlets throughout an entire mission, that is to say, through several sets of Mach number, altitude, and angle of attack, together with the geometric and aerodynamic constraints. As a first step, optimizations are focused on the improvement of current inlet designs for one upstream flow condition. Thereafter, the optimization of inlets throughout several flow conditions is investigated. The main optimization objective is to maximize the total pressure recovery coefficient η of the inlet, which represents its aerodynamic performance at each Mach number encountered.

An automated optimization loop was developed to optimize a baseline inlet originally designed and tested at the Institute of Theoretical and Applied Mechanics (ITAM) in March 1996. To keep approximately the same external cowl drag as the experimental inlets, the cowl shape is fixed, whereas the three

Received Jan. 9, 1998; revision received April 25, 1998; accepted for publication May 6, 1998.

*Engineer; currently at Aerospatiale, Missiles, Center for Computational Design, Les Mureaux, France.

†Professor, Department of Mechanical and Aerospace Engineering, Center for Computational Design. Associate Fellow AIAA.

‡Research Associate, Department of Computer Science, Center for Computational Design.

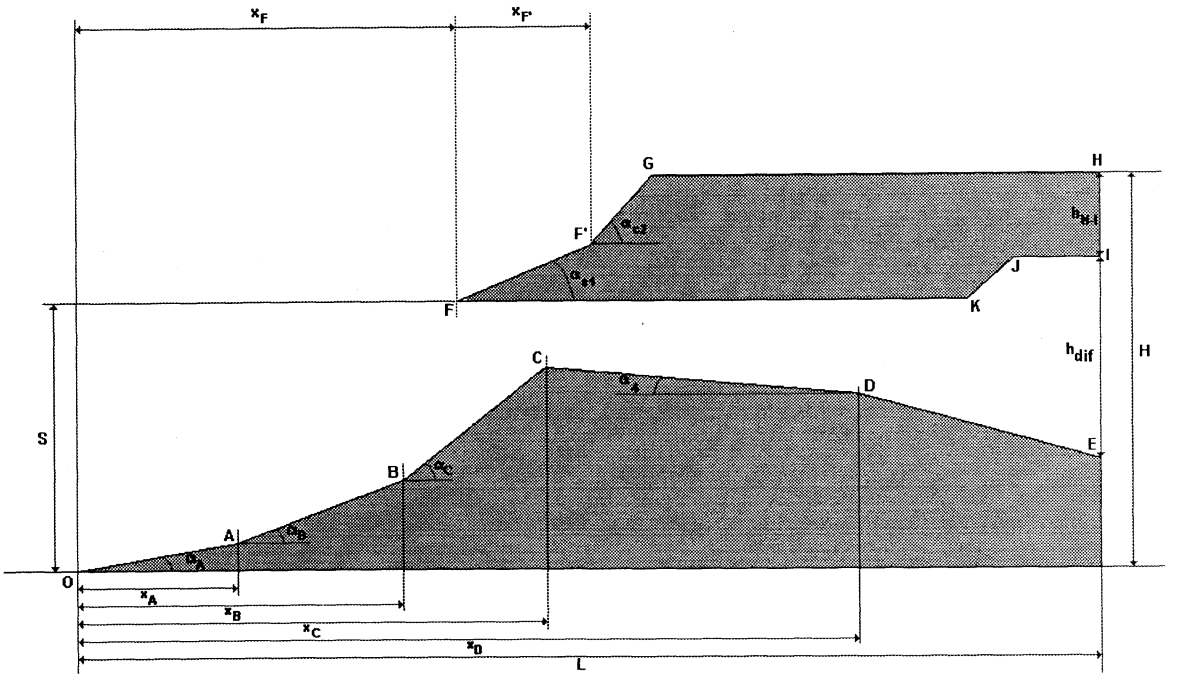

Fig. 1 Geometry model.

compression ramps are optimized. [High total pressure recovery can easily be achieved at the expense of increased cowl drag. Therefore, it is appropriate to maintain a fixed cowl (and, therefore an approximately constant cowl drag) to demonstrate the capability for improving η through automated optimization.] The optimization process that was developed integrates a semiempirical flow solver with an improved GA. Because of computer power limitations and the global optimization time, a full Navier–Stokes solver cannot be used within the automated process. The efficient simple analysis tool used within the optimization loop is Outil de Conception d'Entrées d'Air Supersoniques (OCEAS), which is a fast and accurate semiempirical flow solver. However, in order to validate the results from the automated design loop, the flowfield of the optimized inlets is also computed using a Reynolds-averaged Navier–Stokes code.

II. Geometry Model

In March 1996, the Institute of Theoretical and Applied Mechanics (ITAM), in Novosibirsk, Russia, performed an experimental investigation of two-dimensional, mixed compression, high-speed inlets. Figure 1 presents the geometry model.

A. Description of ITAM Inlets

This geometry model was designed by ITAM to achieve high performance for Mach numbers between 2.5 and 5. The geometries were characterized by two external compression ramps (O-B) and one internal ramp (B-C). The throat was located after the third ramp at point C. The internal shape of the cowl was horizontal, and the diffuser end fixed. During experimental testing, several ramp configurations combined with two different cowls were investigated. Reference to these artifacts will be done using denomination "cowl 1" or "cowl 2" for the cowls, and "insert 1" to "insert 5" for the ramp configurations.

B. Description of Optimization Geometry Model

The same model is used to define the inlet geometry for the optimization. The cowl shape remains fixed to avoid any significant external aerodynamical changes in the drag or lift. Both cowls tested at ITAM are investigated. Only the three-ramp shape is used to maximize the total pressure recovery, resulting in a six-degree-of-freedom optimization. All of the parameters that define the geometry can be seen on Fig. 1. The optimized parameters are x_A, X_B, x_C, α_A, α_B, and α_C. ITAM investigated two different Mach numbers: 3.5 and 5. These Mach numbers are considered for single-condition optimization. Mission optimization is performed over the Mach number range from 2.5 to 5.

III. Optimization Algorithm

Among the global optimizers, GAs demonstrated their effectiveness in very diversified engineering problems.[20,21,36] GAs are search algorithms that mimic the behavior of natural selection to solve given problems.[5] These algorithms first generate a random collection (population) of potential solutions (individuals or candidates). Using mutations and recombinations (crossover) operations, they evolve the population toward better solutions, as individuals become adapted to the problem faced. The GA that will be used belongs to the same theory; nevertheless, it has several improvements that make it more efficient and reliable. Genetic algorithm for design optimization (GADO) is this special GA. A preliminary version of GADO has been used in this research, and did not include all of the modules described in the thesis.[36]

Classical GAs make the formal population evolve generation after generation, losing track of the history information along the search. GADO similarly mutates the population by replacing individuals with "newborns"; however, replaced individuals are stored and used to reseed the population or guide the optimization process (all of these modules will be described later). Furthermore, GADO uses a vector representation of individuals. Each individual represents a parametric description of the inlet, with each parameter taking on a value in some continuous interval. Each individual has a fitness, which is based upon the sum of the objective function and the penalty function. The objective function is the heart of the optimization process: it is defined as the function to minimize. For one upstream flow condition optimization, the objective function is equal to the total pressure recovery coefficient. In the case of mission optimization, the objective function is more complicated and will be discussed later. The value of the penalty function is proportional to the amplitude of the constraint violations for the considered inlet. This function has been tailored to guide the GA toward feasible regions. The objective function will be evaluated only in the event that no constraints

have been violated. That is to say that the penalty function is equal to zero.

GADO includes several specific implementations and modules that have been incorporated with a view to accelerate the convergence of the search process toward the global optimum. This GA has demonstrated its effectiveness in several engineering optimization problems.[36] Moreover, it has proved to be quicker and more likely to converge toward the global optimum than classical GAs, gradient-based methods, or random probe processes. The power of this optimization algorithm stems from the fact that it combines advantages from both nongradient and gradient-based search algorithms. The improved GA uses the search quality of nongradient-based algorithms while simulating gradient based methods when it is near the global optimum. With a view to ensuring the high performance of GADO, Sec. VII will present a comparison with a gradient-based method.

IV. Flow Solvers

The purpose of the automated optimization loop is to maximize the total pressure recovery coefficient of a two-dimensional high-speed missile inlet. A flow solver is needed to compute the inlet flowfield. The most accurate tools available are Reynolds-averaged Navier–Stokes flow solvers; however, they are too CPU-intensive to be included in a GA-based optimization that requires at least 5000 flowfield computations. Therefore, a simple, fast, and accurate flow solver is used within the optimization loop, whereas a Navier–Stokes analysis tool is used to verify final results. The efficient simple flow solver is named OCEAS.

A. OCEAS

OCEAS was developed at Aerospatiale, Missiles (France), to assist engineers in the aerodynamic design of missile inlets.[37] It is a semiempirical flow solver that uses simple but accurate physical models that require little CPU time. When the inlet is started, that is to say, when the flowfield is supersonic after the cowl entrance until a certain point within the inlet's duct, the supersonic and subsonic region of the flowfield are separated by an approximately normal shock. The supersonic flowfield is calculated first. Shocks are computed by solving the Rankine–Hugoniot equations. Expansion fans are modeled using the Prandtl–Meyer formula and mass flow rate conservation. Boundary layers can also be modeled by their displacement effect; however, this was not used in this study. The subsonic flowfield is not computed, but losses within the diffuser are approximated by simple empirical formulas that take sudden expansion, friction and separation at the throat into consideration. The maximum value of η is achieved when the normal shock is located at the throat. Therefore, OCEAS computes only the flowfield corresponding to this particular position of the normal shock. Each computation requires only 2 CPU seconds using a DEC ALPHA 2100 workstation. This computation time is far less than the time required for one Navier-Stokes computation.

The accuracy of OCEAS is demonstrated for the baseline (nonoptimized) inlets in Table 1, where the predicted and experimental total pressure recovery coefficient η and mass flow rate ε are shown. One can see that OCEAS accurately predicts these inlet performance parameters, with an error of 1–8% in η, and 5–6% in ε.

B. General Aerodynamic Simulation Program

The computational fluid dynamics Navier–Stokes solver used is the General Aerodynamic Simulation Program (GASP), a code developed by Aerosoft, Inc.[38] It is a two- or three-dimensional Reynolds-averaged Navier–Stokes solver that employs high-resolution upwind schemes for the invicid fluxes and central differencing for the viscous fluxes. An implicit two-factor approximate factorization (AF) scheme is used in the spanwise plane, and relaxation sweeping is used in the streamwise direction.

A Navier–Stokes computation of a supersonic inlet is time consuming because the back pressure at the end of the subsonic diffuser is unknown and must be determined using a root search iteration until the critical operating point is reached. Moreover, when the back pressure is close to the critical value, the shock system moves very slowly and a long CPU time is required to ensure the shock stability. One flowfield computation requires typically 4 CPU hours on a DEC ALPHA 2100 workstation for an 85×181 grid. Reaching the critical regime requires 5–7 computations, leading to an overall computational time of about 30 CPU hours.

GASP computations have been performed to verify the results obtained by the automated optimization loop using OCEAS. Computation of the original inlets tested at ITAM have also been performed, and are presented in Table 1. One can see the accuracy of the simulation for all experimental inlets. Actually, the computed total pressure recovery and mass flow rate coefficients are within 2 and 4% of the experiment, respectively.

V. Constraints

Through the penalty function, several constraints, related to different specifications and requirements, are implemented. They must be designed to guide the GA toward feasible regions. Simple geometrical constraints are designed to ensure the reality of the inlet shape, i.e., that the parameters describe a real inlet. The unstart constraint is used to verify the starting Mach number of the inlet. ITAM experimental inlets are unstarted at Mach 2, but are started at Mach 3.5. Therefore, the optimized inlets are required to start at Mach 3. This criterion is based on the Mach number value at the cowl entrance and on the contraction ratio of the inlet (ratio of the entrance cowl section to the throat section). For a given cowl entrance, the contraction ratio must be lower than the contraction ratio that would give Mach 1 at the throat from an isentropic compression. The first ramp angle must be greater than 1 deg for manufacturing purposes. The cross-sectional area at the throat must be the minimum within the whole duct from entrance to exit. Additional constraints arise when considering mission optimization and they will be discussed later.

VI. Optimization for One Upstream Flow Condition

A. Optimization Results

The automated optimization loop has been performed for the two flow conditions: Mach 3.5 and Mach 5. A complete op-

Table 1 Experimental data and computations of baseline inlets

Mach number	Inlet	Quantity	Experimental data	OCEAS	Difference 1, %[a]	GASP	Difference 2, %[b]
5	Insert 1 cowl 1	η	0.150	0.162	8	0.153	2
		ε	0.800	0.841	5	0.806	1
5	Insert 5 cowl 2	η	0.135	0.134	1	0.137	1.5
		ε	0.925	0.982	6	0.962	4
3.5	Insert 4 cowl 2	η	0.375	0.371	1	0.378	1
		ε	0.800	0.841	5	0.802	0.5

[a]Gap between OCEAS prediction and experimental data.
[b]Gap between GASP prediction and experimental data.

Table 2 Single flow condition optimization results

Mach number	Cowl	Quantity	Baseline[a]	Optimized (OCEAS)[b]	Improvement, %[c]	Optimized (GASP)[d]	Difference, %[e]
5	1	η	0.162	0.193	18	0.186	3.8
		ε	0.841	0.999	19	0.995	19
5	2	η	0.134	0.217	62	0.183	18.5
		ε	0.982	1.000	2	1.000	0.0
3.5	2	η	0.371	0.484	30	0.441	9.8
		ε	0.841	0.916	9	0.960	9

[a]Best baseline inlet value of aerodynamic coefficient.
[b]OCEAS computation of the optimized inlet.
[c]Improvement when comparing OCEAS simulation to baseline value.
[d]GASP computation of the optimized inlet.
[e]Difference between OCEAS and GASP computation.

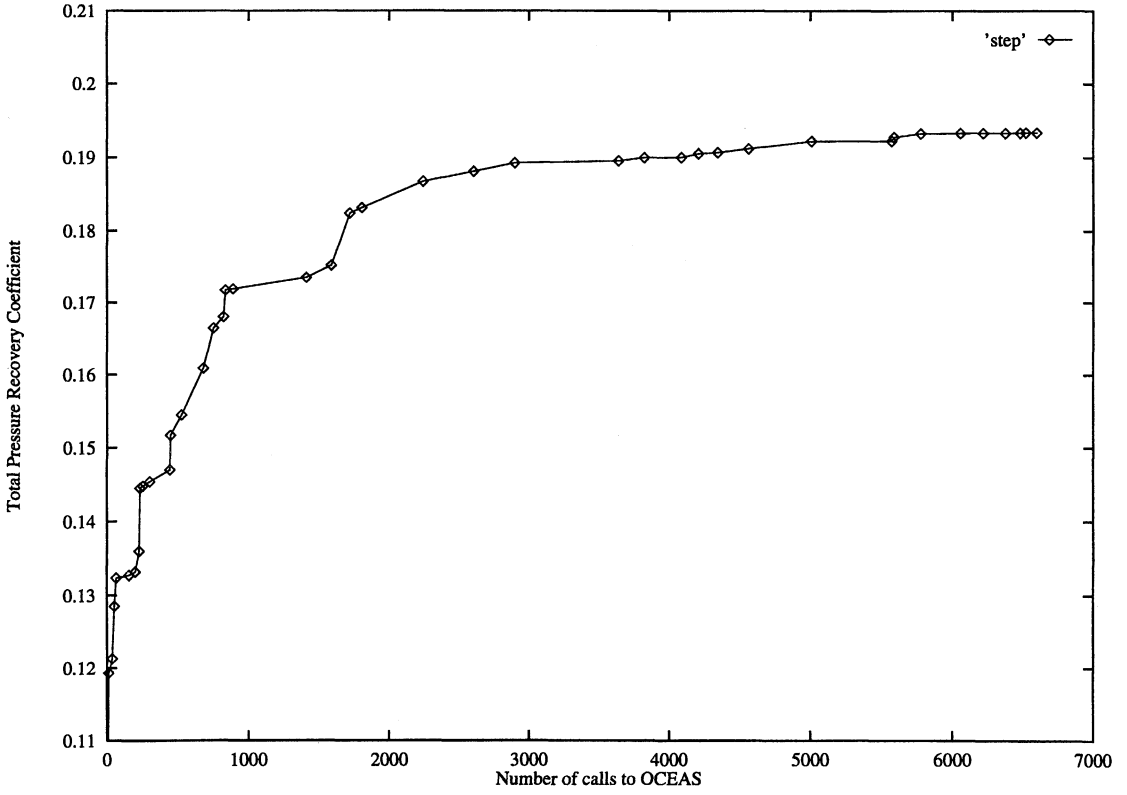

Fig. 2 Convergence history for optimization at Mach 5 using cowl 1.

timization requires approximately 25,000 iterations of GADO, in which there are 7000 calls to OCEAS. Because this flow solver takes 2 CPU seconds to compute the maximum value of the aerodynamic coefficients, and the computation of the penalty function is about 5×10^{-2} CPU seconds, the total time to complete one entire optimization is about 5 CPU hours on a DEC ALPHA 2100 workstation.

For conditions at Mach 5, the optimization process has been applied using both cowls. For conditions at Mach 3.5, the optimization process has been applied only with cowl 2. Figure 2 presents the convergence history of one optimization process. Table 2 shows the optimization results compared to the experimental baseline. Significant improvements of the baseline designs have been achieved using GADO coupled with the OCEAS flow solver. The optimization process using cowl 2 at Mach 5, gives a total pressure recovery coefficient of 0.217, which is 62% higher than the best experimental inlet using cowl 2 (insert 5 cowl 2). For Mach 3.5 conditions, the optimum design using cowl 2 has a total pressure recovery of 0.484, which represents a 29% improvement.

In addition to these significant improvements, the mass flow rate of the optimized inlets are much higher than the experimental ones. We define the term *adapted Mach number* as the Mach number of the upstream flow for which the shock issuing from the leading edge of the first ramp intersects the apex of the cowl. The optimization process designs inlets that have an adaptive Mach number closer to the upstream Mach number. The experimental inlets have an adapted Mach number higher than 5.5, which results in losses in the mass flow rate spilt out of the inlet for Mach numbers under 5.5.

The optimization is evaluating very different configurations throughout the search process. As GAs are stochastic methods, it is not possible to see one definite trend in the convergence of the shape of the inlet. Actually, GADO keeps jumping from one design family to another as it finds more promising design regions. This is a direct consequence of the fact that there is an infinity of geometry configurations that have an adapted Mach number equal to the upstream Mach number.

B. Verification

The three experimental inlet configurations, as well as the three optimized inlet designs were computed using the Navier–Stokes analysis tool described previously. These computations were performed using a two-dimensional mesh of 85 points by 181 points composed of two different blocks. The two-equation Chien k-ε turbulence model is used. The inner

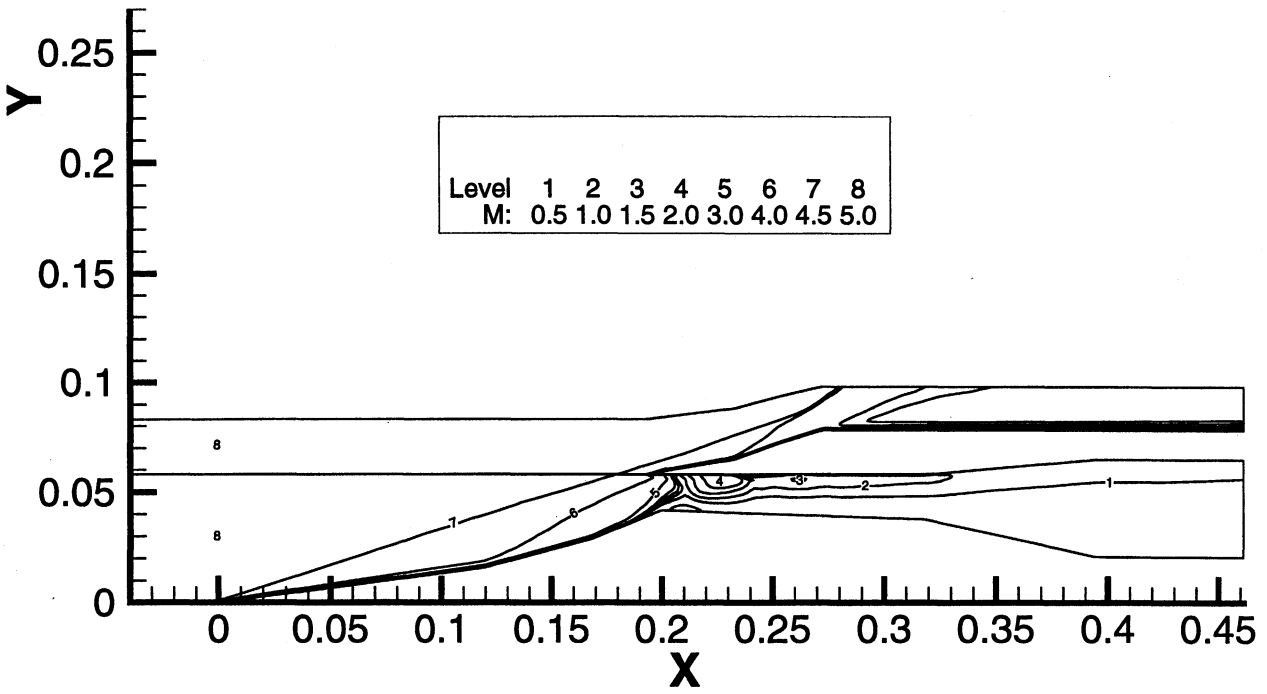

Fig. 3 Computed Mach number contours of experimental inlet using insert 5 and cowl 2 at Mach 5.

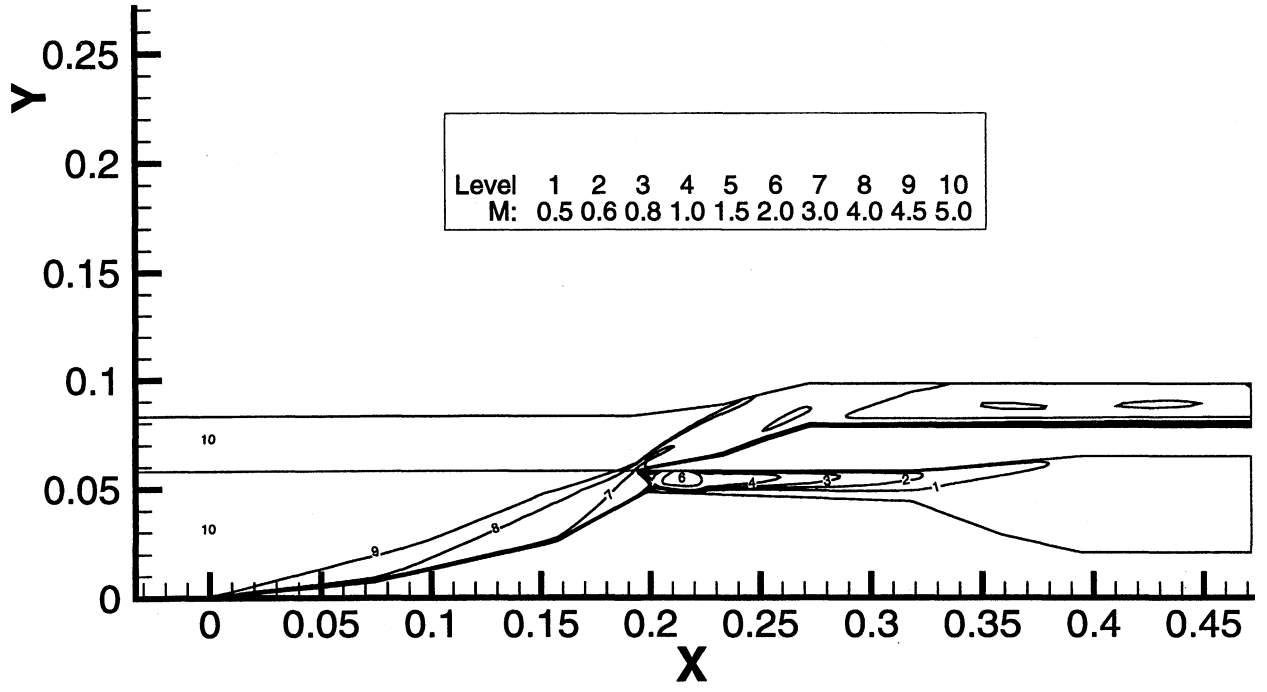

Fig. 4 Computed Mach number contours of optimized inlet at Mach 5 using cowl 2.

block extends from the centerbody leading edge, through the internal channel, to the diffuser ending. The outer block covers the flowfield from the incoming freesteam through the external surface of the cowl. Figure 3 shows the Mach number contours of the flowfield obtained for the experimental inlet using insert 5 with cowl 2. Figure 4 shows the Mach number contours of the flowfield obtained for the optimized inlet at Mach 5 using cowl 2. Root searches for the critical value of total pressure recovery coefficient and mass flow rate, give the results that are gathered in Tables 1 and 2. Table 2 compares the aerodynamic coefficient values obtained by OCEAS and GASP. As can be seen in every instance, the difference between the predictions using OCEAS and GASP is small compared to the improvement achieved using OCEAS in the automated optimization loop. This confirms the accuracy of the optimized inlets. The improvements achieved in total pressure recovery are between 20 and 40%, which represent significant increases of this aerodynamic coefficient.

C. Discussion

The automated optimization loop developed so far has proven to be very efficient in designing an optimum two-dimensional inlet for one upstream flow condition. Moreover, the improvement achieved has been confirmed by the Navier–Stokes code. However, the optimized inlets obtained have significantly different shapes, depending on the design Mach number. Because missiles are designed to fly through several flow conditions (different Mach numbers and alti-

tudes), it should be interesting to see how an inlet optimized for Mach 5 will perform when flying at Mach 3.5 and vice versa. Furthermore, it should be interesting to compare the performance of all the inlets considered through an entire mission. Figure 5 gathers the performance curve of the experimental and optimized inlets. These performance curves are defined as the value of the total pressure recovery coefficient η corresponding to each Mach number of the mission. Values of this aerodynamic coefficient are computed using OCEAS. As one can see, inlets optimized for a specific Mach number have higher values of the total pressure recovery than the other inlets around this Mach number. But their performance falls quickly for other Mach numbers of the mission. For example, the inlet optimized at Mach 3.5 is the best performing inlet from Mach 2.5 to Mach 4. However, its performance deteriorates from Mach 4 to Mach 5 faster than any other inlet. It is evident that an inlet cannot be optimized for an entire mission by focusing on one flow condition only. Actually, the inlet will perform badly on the other mission points. Thereby, several upstream flow conditions have to be taken into consideration, as will be described in Sec. VIII.

VII. Comparison with a Gradient-Based Method

With a view to demonstrate the capability and performance of the optimization tool used in the previous section, a comparison with a gradient-based algorithm has been performed. The method is C code for feasible sequential quadratic programming (CFSQP).[39] Several settings have been used with a view to achieve the best performance of the gradient-based method. CFSQP converges significantly faster than GADO but is not able to find the global optimum. Actually, only 20 to 50 iterations of the optimization algorithm are necessary. This kind of optimization software needs a starting point. When launched from an experimental design point (insert 5, cowl 2, which has $\eta = 0.134$), CFSQP achieves an improvement of 20% ($\eta = 0.160$), which can be compared to the 62% ($\eta = 0.217$) improvement achieved by GADO. Moreover, when launched from the optimum found by the GA, no further improvement was achieved. A random multistart was also carried out, but without any further improvement. This comparison shows the reliability and the merit of the GA used.

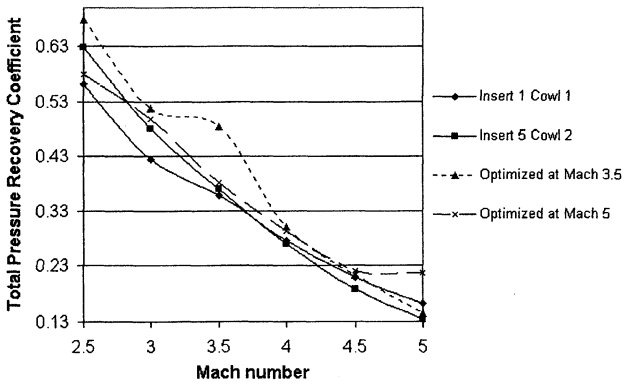

Fig. 5 Performance of each inlet throughout entire mission.

VIII. Mission Optimization

To effectively perform the optimization over an entire mission, the constraints, objectives, and requirements of a high-speed missile's mission must be investigated. The problem of designing an optimum inlet for an entire mission can be approached from two different ways. At first glance, the optimization can become multiobjective. However, this strategy does not seem to be suitable to the problem faced, because it leads to several pareto optimum inlets and is time consuming. (Each pareto design is optimal in the sense that no improvement can be achieved in one objective function that does not lead to degradation in at least one of the remaining functions.) The right solution is to combine the several objectives into a single one. Actually, if all of the mission requirements and constraints are known, then, based on computational and experimental data, it is possible to design a target curve $\eta_{tgt} = f(\text{Mach})$ for the entire mission. This curve relies on the given motor and the particular mission to be performed. Thereby, the optimization process will remain uniobjective and the purpose will be to minimize the gap between optimized inlet curve and the target curve.

A. Definition of a Mission for High-Speed Missile

A mission for a supersonic missile can be divided into roughly three different stages. Figure 6 presents a mission overview. The first stage is called acceleration. Just after being launched, the missile must accelerate and reach its cruise altitude and speed. During this stage it must use a minimum amount of fuel, to be able to cover the greatest distance during the cruise period. Therefore, the missile must have the greatest thrust possible. To satisfy this objective, the mass flow rate must be maximum. At this stage, the total pressure recovery is not a constraint because its value is typically high. The next step is the cruise stage. During this period, the objective is to cover the greatest distance as possible. Therefore, the total pressure recovery coefficient must be maximized while the mass flow rate must be at least equal to an acceptable minimum. This acceptable value must be defined with a view to

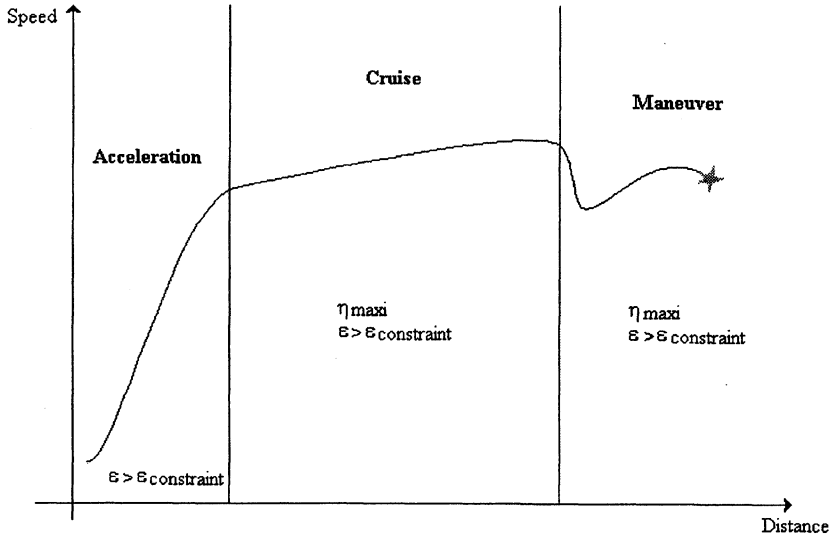

Fig. 6 Mission profile.

satisfy motor constraints. As the missile is reaching its target, it enters the maneuver stage. At this point the dominating parameter is still the total pressure recovery. Its value must be maximized while the mass flow rate must be greater than another acceptable minimum value.

To summarize, the total pressure recovery has to be maximized for all mission stages, whereas the mass flow rate must be kept greater than acceptable values. As previously investigated, it is not possible to maximize the total pressure recovery coefficient for the entire mission without making some compromise between all mission points. Thereby, regarding the particular mission requirement and the given motor performance, a target performance curve must be designed with a view to guide the optimization process.

B. Optimization Strategy

The target curve will give, for all of the mission stages, i.e., for all flow conditions encountered by the missile, the value of the total pressure recovery coefficient that best fits the given motor and mission profile. However, the target value will be slightly overestimated to keep all optimized values below it. This curve is noted $\eta_{tgt} = f(\text{Mach})$. In addition to this target curve, constraints on the mass flow rate value must be met throughout several stages, creating another curve called the constraint curve and noted $\varepsilon_{\text{cons}} = g(\text{Mach})$. The goal of the automated optimization loop will be to minimize the gap between the performance curve of the currently analyzed inlet and the target curve, while taking into consideration the mass flow rate contraints. As before, OCEAS will be used during the optimization process, whereas GASP will be used to verify the optimal design.

C. Optimization Results

The optimization strategy described previously has been applied to a virtual mission built upon extrapolation of the inlet baseline test results. A total of 30,000 iterations of the optimization algorithm are necessary to achieve convergence, which means 9000 calls to the objective function. As six flowfield computations are needed to calculate the objective function, a total of 54,000 calls to OCEAS were performed during the optimization. Therefore, the overall computation time is about 30 CPU hours on a DEC alpha 2100 workstation. Figure 7 presents the optimization results compared to the target curve and the experimental inlet performance (insert 5 cowl 2, which proved to have the best overall performance throughout the mission). Figure 8 shows that the mass flow rate of the optimized inlet meets or exceeds the constraint curve at every point. Figure 9 presents the comparative plot of the performance of inlets optimized for one flight condition and for the entire mission. This figure shows the improvement made by taking into consideration all of the mission's conditions to lead to a better performing inlet for the overall range of Mach num-

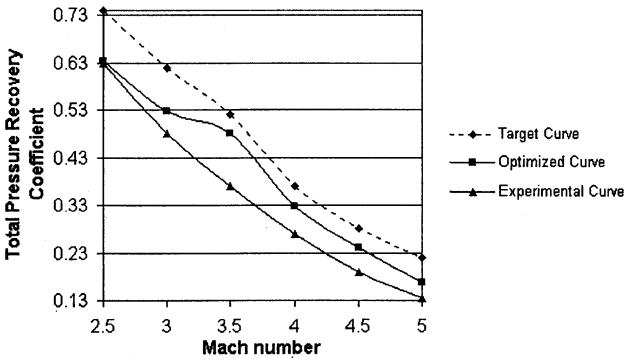

Fig. 7 Total pressure recovery coefficient vs Mach number.

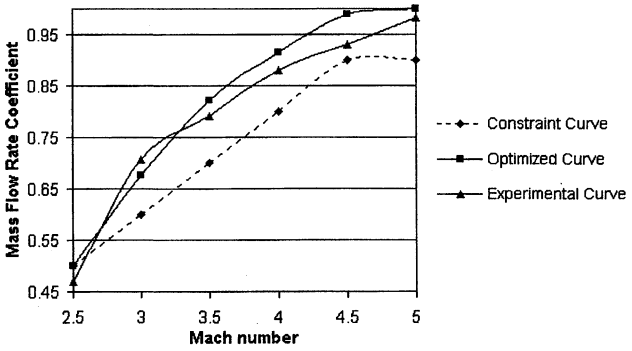

Fig. 8 Mass flow rate coefficient vs Mach number.

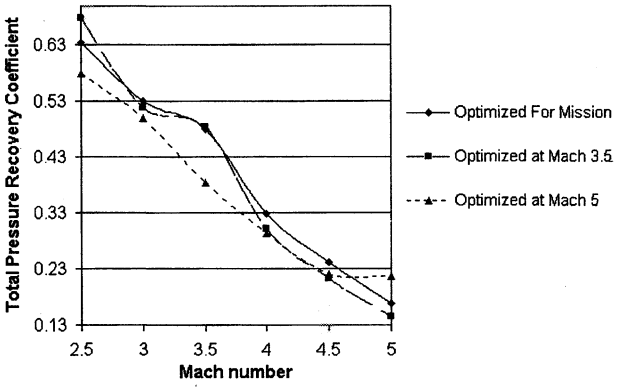

Fig. 9 Total pressure recovery coefficient vs Mach number for optimized inlets.

Table 3 Mission optimization results

Mach number	Quantity	Baseline[a]	Optimized (OCEAS)[b]	Improvement, %[c]	Optimized (GASP)[d]	Difference, %[e]
2.5	η	0.629	0.635	1.0	——	——
	ε	0.469	0.500	6.6	——	——
3.0	η	0.480	0.529	10.2	——	——
	ε	0.706	0.677	−4.1	——	——
3.5	η	0.371	0.480	29.4	0.410	17.1
	ε	0.792	0.821	3.7	0.89	7.7
4.0	η	0.270	0.327	21.1	——	——
	ε	0.880	0.916	4.1	——	——
4.5	η	0.189	0.241	27.5	——	——
	ε	0.930	0.989	6.3	——	——
5.0	η	0.134	0.168	25.4	0.163	3.1
	ε	0.982	1.000	1.8	1.000	0.0

[a]Best baseline inlet value of aerodynamic coefficient.
[b]OCEAS computation of the mission optimized inlet.
[c]Improvement when comparing OCEAS simulation to baseline value.
[d]GASP computation of the mission optimized inlet.
[e]Difference between OCEAS and GASP computation.

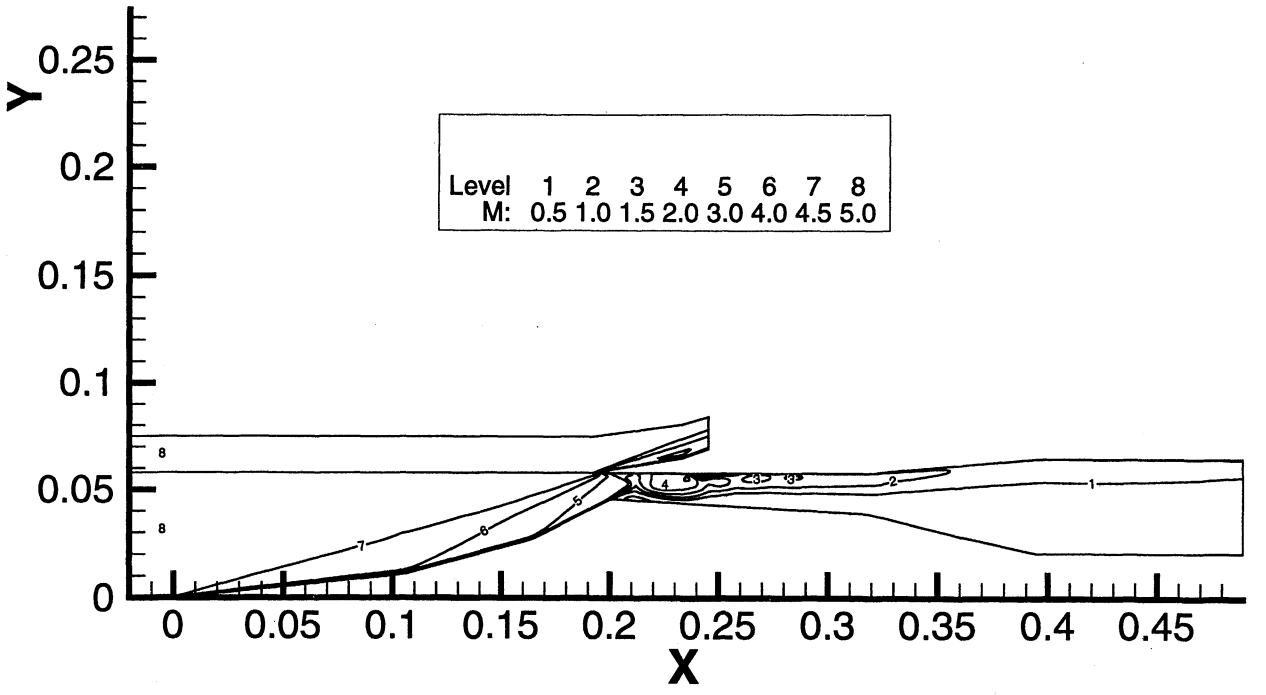

Fig. 10 Computed Mach number contours at Mach 5 for mission-optimized inlet.

ber. Table 3 gathers the comparative results of the best performing experimental inlet and the optimum inlet. One can see the significant improvement achieved by the automated optimization loop. An average 20% improvement is obtained by OCEAS.

D. Verifications

Results obtained for Mach 5 and Mach 3.5 have been verified using the same mesh and flowfield computation as the one described in Sec. VI.B (except for the upper zone that has been shortened). Figure 10 shows the Mach-number contours of the mission optimized inlet at Mach 5 conditions. The computational values achieved are shown in Table 3. Because the gap between the predicted OCEAS values and the ones computed by GASP is always significantly less than the improvement made, the optimization results are confirmed.

IX. Conclusions

An automated optimization loop for two-dimensional high-speed missile inlets has been developed. This new technique combines an improved GA and a semiempirical flow solver. Very successful results have been achieved using this automated process for optimization of a two-dimensional inlet for one upstream flow condition and for multiple upstream conditions, i.e., an entire mission. Actually, improvement up to 40% in total pressure recovery compared to the baseline inlet configurations has been achieved and confirmed by a Navier–Stokes solver for the single-point optimization. Furthermore, the optimization strategy for designing inlets throughout an entire mission has showed improvement up to 20% for each Mach number encountered.

Future work is oriented toward two areas. The first one is focused on the development of optimization strategy to design three-dimensional inlets. Performance during side-slip is then of special interest. The second one is to develop multidisciplinary optimization methods involving several simulation tools to design the missile as a whole, taking into consideration the conceptual and optimization aspects.

Acknowledgments

Technical and financial support for this research was provided by Aerospatiale, Missiles, and the Hypercomputing and Design Project supported by the Advanced Research Projects Agency of the Department of Defense through Contract ARPA-DABT 63-93-C-0064. The content of the information herein does not necessarily reflect the position of the government and official endorsement should not be inferred. We would like to thank Haym Hirsh, Xavier Montazel, Vijay Shukla, Donald Smith, and Gecheng Zha for their invaluable assistance in this research.

References

[1]Hicks, R. M., and Henne, P. A., "Wing Design by Numerical Optimization," *Journal of Aircraft*, Vol.15, No.7, 1978, pp. 407–412.

[2]Ta'asan, S., "Trends In Aerodynamics Design Optimization: A Mathematical Viewpoint," AIAA Paper 95-1731, June 1995.

[3]Arian, E., and Ta'asan, S., "Analysis of the Hessian for Aerodynamic Optimization: Inviscid Flow," Inst. for Computer Applications in Science and Engineering, Rept. 96-28, NASA Langley Research Center, Hampton, VA, April 1996.

[4]Jameson, A., "Optimum Aerodynamic Design Using CFD and Control Theory," AIAA Paper 95-1729, June 1995.

[5]Joshi, B., Morris, D., White, N., and Unal, R., "Optimization of Operation Resources via Discrete Event Simulation Modeling," AIAA Paper 96-4181, Sept. 1996.

[6]Whitley, D., "A Genetic Algorithm Tutorial," Dept. of Computer Science, TR CS-93-103, Colorado State Univ., Fort Collins, CO, Nov. 1993.

[7]Goldberg, D. E., *Genetic Algorithms in Search, Optimization, and Machine Learning*, Addison–Wesley, Reading, MA, 1989.

[8]Ta'asan, S., Kuruvila, G., and Salas, M., "Aerodynamic Design and Optimization in One Shot," AIAA Paper 92-0025, Jan. 1992.

[9]Limache, A. C., "Inverse Method for Airfoil Design," *Journal of Aircraft*, Vol. 32, No. 5, 1995, pp. 1001–1011.

[10]Prasanth, R. K., and Whitaker, K. W., "Neuromorphic Approach to Inverse Problems in Aerodynamics," *AIAA Journal*, Vol. 33, No. 6, 1995, pp. 1150–1152.

[11]Bock, K. W., "Aerodynamic Design By Optimization," Dornier Luftfahrt GmbH, Friedrichshafen, Germany.

[12]Pandya, M. J., and Baysal, O., "Gradient-Based Aerodynamic Shape Optimization Using Alternating Direction Implicit Method," *Journal of Aircraft*, Vol. 34, No. 3, 1997, pp. 346–352.

[13]Sadrehaghighi, I., Smith, R. E., and Tiwari, S. N., "Grid Sensitivity and Aerodynamic Optimization of Generic Airfoil," *Journal of Aircraft*, Vol. 32, No. 6, 1995, pp. 1234–1239.

[14]Burgreen, G. W., and Baysal, O., "Three-Dimensional Shape Optimization Using Discrete Sensitivity Analysis," *AIAA Journal*, Vol. 34, No. 9, 1996, pp. 1761–1770.

[15]Cosentino, G. B., and Holst, T. L., "Numerical Optimization Design of Advanced Transonic Wing Design Configurations," *Journal of Aircraft*, Vol. 23, No. 3, 1986, pp. 192–199.

[16]Hutchison, M. G., Unger, E. R., Mason, W. H., Grossman, B., and Haftka, R. T., "Variable-Complexity Aerodynamic Optimization of a High-Speed Civil Transport Wing," *Journal of Aircraft*, Vol. 31, No. 1, 1994, pp. 110–116.

[17]Dodbele, S. S., "Design Optimization of Natural Laminar Flow Bodies in Compressible Flow," NASA CR 4478, Dec. 1992.

[18]Newman, J. C., Taylor, A. C., and Burgreen, G. W., "An Unstructured Grid Approach to Sensitivity Analysis and Shape Optimization Using the Euler Equations," AIAA Paper 95-1646, June 1995.

[19]Sly, S., Marconi, F., Ogot, M., Pelz, R., and Siclari, M., "Stochastic Optimization Applied to CFD Shape Design," AIAA Paper 95-1647, June 1995.

[20]Obayashi, S., Yamaguchi, Y., and Nakamura, T., "Multiobjective Genetic Algorithm for Multidisciplinary Design of Transonic Wing Platform," *Journal of Aircraft*, Vol. 34, No. 5, 1997, pp. 690–693.

[21]Yamamoto, K., and Inoue, O., "Application of Genetic Algorithm to Aerodynamic Shape Optimization," AIAA Paper 95-1650, June 1995.

[22]Eyi, S., Lee, D., Rogers, S. E., and Kwak, D., "High Lift Design Optimization Using Navier–Stokes Equations," *Journal of Aircraft*, Vol. 33, No. 6, 1996, pp. 499–504.

[23]Knight, D. D., "Automated Optimal Design Using CFD and High Performance Computing," *Lecture Notes in Computer Science*, edited by J. Palma and J. Dongarra, Vol. 1215, 1997, pp. 198–221.

[24]Baysal, O., and Eleshaky, M. E., "Aerodynamic Design Optimization Using Sensitivity Analysis and Computational Fluid Dynamics," *AIAA Journal*, Vol. 30, No. 3, 1992, pp. 718–725.

[25]McQuade, P. D., Eberhardt, S., and Livne, E., "CFD-Based Aerodynamic Approximation Concepts Optimization of a Two-Dimensional Scramjet Vehicle," *Journal of Aircraft*, Vol. 32, No. 2, 1995, pp. 262–269.

[26]Zha, G.-C., Smith, D., Schwabacher, M., Rasheed, K., Gelsey, A., and Knight, D., "High Performance Supersonic Missile Inlet Design Using Automated Optimization," AIAA Paper 96-4142, Sept. 1996.

[27]Shukla, V., Gelsey, A., Schwabacher, M., Smith, D., and Knight, D., "Automated Design Optimization for the P2 and P8 Hypersonic Inlets," *Journal of Aircraft*, Vol. 34, No. 2, 1997, pp. 228–235.

[28]Hussaini, M. M., and Korte, J. J., "Investigation of Low-Reynolds-Number Rocket Nozzle Design Using PNS-Based Optimization Procedure," NASA TM 110295, Nov. 1996.

[29]Borovikov, A., Gavriliouk, V., Khokhlov, A., Lanshin, A., Sobatchkine, A., and Sokolov, V., "Optimal Nozzle Profiling for "Orel-2-1" Transport System," AIAA Paper 96-2685, July 1996.

[30]Dulikravich, G. S., Buss, R. N., Strang, E. J., and Lee, S., "Aerodynamic Shape Optimization of Hypersonic Missiles," AIAA Paper 90-3073, Aug. 1990.

[31]Sobieszczanski-Sobieski, J., and Haftka, R. T., "Multidisciplinary Aerospace Design Optimization: Survey of Recent Developments," AIAA Paper 96-0711, Jan. 1996.

[32]Alexandrov, N., and Dennis, J. E., Jr., "Multilevel Algorithms for Nonlinear Optimization," Inst. for Computer Applications in Science and Engineering, Rept. 94-53, NASA Langley Research Center, Hampton, VA, June 1994.

[33]Gelsey, A., "Intelligent Automated Quality Control for Computational Simulation," *Artificial Intelligence for Engineering Design, Analysis and Manufacturing*, March 1995, pp. 387–400.

[34]Housner, J., "Rapid Modeling Assembly and Simulation in Design Optimization," NASA Langley Research Center, Hampton, VA.

[35]Otto, J. C., Landman, D., and Patera, A. T., "A Surrogate Approach to the Experimental Optimization of Multi-Element Airfoils," AIAA Paper 96-4138, Sept. 1996.

[36]Rasheed, K., "GADO: A Genetic Algorithm for Continuous Design Optimization," Ph.D. Dissertation, Dept. of Computer Science, Rutgers Univ., Piscataway, NJ, Jan. 1998.

[37]Lacau, R. G., Ganero, P., and Gaible, F., "Computation of Supersonic Intakes," AGARD Special Course on Missiles Aerodynamics, AGARD Rept. 804, 1994.

[38]"GASP, General Aerodynamic Simulation Program Version 3 User's Manual," Aerosoft, Inc., Blacksburg, VA, May 23, 1996.

[39]Lawrence, C., Zhou, J. L., and Tits, A. L., "CFSQP Version 2.3: A C Code for Solving Constrained Nonlinear Optimization Problems, Generating Iterates Satisfying All Inequality Constraints," Electrical Engineering Department and Institute for Systems Research, TR 94-16rl, Univ. of Maryland, College Park, MD, Nov. 1994.